Point forces in elasticity equation and their alternatives in multi dimensions

Peng, Q.; Vermolen, F.J.

DOI
10.1016/j.matcom.2022.03.021

Publication date
2022

Document Version
Final published version

Published in
Mathematics and Computers in Simulation

Available online at www.sciencedirect.com
ScienceDirect
Mathematics and Computers in Simulation 199 (2022) 182–201
MATHEMATICS AND COMPUTERS IN SIMULATION
www.elsevier.com/locate/matcom

Original articles

Point forces in elasticity equation and their alternatives in multi dimensions

Q. Peng[a,b,c,*], F.J. Vermolen[c,b]

[a] Mathematical Institute, Leiden University, Niels Bohrweg 1, 2333 CA Leiden, The Netherlands
[b] Delft Institute of Applied Mathematics, Delft University of Technology, Mekelweg 4, 2628 CD Delft, The Netherlands
[c] Computational Mathematics Group, Department of Statistics and Mathematics, Hasselt University, Agoralaan Gebouw D, 3590 Diepenbeek, Belgium

Received 2 April 2021; received in revised form 14 March 2022; accepted 23 March 2022
Available online 4 April 2022

Abstract

Deep dermal wounds induce skin contraction as a result of the traction forcing exerted by (myo)fibroblasts on their immediate environment. These (myo)fibroblasts are skin cells that are responsible for the regeneration of collagen that is necessary for the integrity of skin We consider several mathematical issues regarding models that simulate traction forces exerted by (myo)fibroblasts. Since the size of cells (e.g. (myo)fibroblasts) is much smaller than the size of the domain of computation, one often considers point forces, modelled by Dirac Delta distributions on boundary segments of cells to simulate the traction forces exerted by the skin cells. In the current paper, we treat the forces that are directed normal to the cell boundary and toward the cell centre. Since it can be shown that there exists no smooth solution, at least not in $\boldsymbol{H^1}$ for solutions to the governing momentum balance equation, we analyse the convergence and quality of approximation. Furthermore, the expected finite element problems that we get necessitate to scrutinize alternative model formulations, such as the use of smoothed Dirac Delta distributions, or the so-called smoothed particle approach as well as the so-called 'hole' approach where cellular forces are modelled through the use of (natural) boundary conditions. In this paper, we investigate and attempt to quantify the conditions for consistency between the various approaches. This has resulted into error analyses in the L^2-norm of the numerical solution based on Galerkin principles that entail Lagrangian basis functions. The paper also addresses well-posedness in terms of existence and uniqueness. The current analysis has been performed for the linear steady-state (hence neglecting inertia and damping) momentum equations under the assumption of Hooke's law.

Keywords: Point forces; Dirac delta distribution; Singular solution; Immersed boundary approach; "Hole" approach; Smoothed particle approach

1. Introduction

Wound healing is a complicated process of a sequence of cellular events contributing to resurfacing, reconstitution and restoration of the tensile strength of injured skin. Significant damage of dermal tissue often leads to skin contraction. If the contraction of the skin near a joint is large then it may result into a decrease of functionality, in these cases, one speaks of a contracture.

* Corresponding author at: Mathematical Institute, Leiden University, Niels Bohrweg 1, 2333 CA Leiden, The Netherlands.
E-mail address: Q.Peng@math.leidenuniv.nl (Q. Peng).

https://doi.org/10.1016/j.matcom.2022.03.021
0378-4754/

In order to improve the patient's quality of life, one aims at reducing the contractile behaviour of the skin. To reduce the severity of the contraction, one needs to know the physiological dynamics and time evolution of the underlying biological mechanisms. According to [8,11,15], the contraction starts developing during the proliferative phase of wound healing. This proliferative phase sets in after the inflammatory phase, in which the immune system is clearing up the debris that resulted from the damage. The proliferative phase usually starts from the second day post-wounding, and commonly lasts two to four weeks. Besides the closure of the epidermis (that is the top layer of skin), the proliferative phase is characterized by ingress of fibroblasts from the surrounding undamaged tissue and differentiation to myofibroblasts, and by the regeneration of collagen by the (myo)fibroblasts. Despite the relatively quick closure of the epidermis, often the restoration of the underlying dermis is still in progress. After closure of the epidermis, the damaged region in the dermis is referred to as a scar instead of a wound. Next to the regeneration of collagen, the (myo)fibroblasts exert contractile forces on their direct surroundings, which will result into contraction of the scar tissue. In human skin, typically volume reductions of 5%–10% are commonly observed [9].

The current manuscript contains an extension of the work in Koppenol [12], which treats a model for the contractile forces exerted by the (myo)fibroblasts. The forces are distinguished into two categories: (1) temporary forces that are exerted as long as the (myo)fibroblasts are actively pulling; and (2) permanent or plastic forces, which are imaginary forces that are introduced to describe the localized plastic deformations of the tissue. This formalism was firstly developed by Vermolen and Gefen [22], and later extended by Boon et al. [5]. The formalism is based on the point forces, which are mathematically incorporated by means of linear combinations of Dirac Delta distributions. The irregular nature of Dirac Delta distributions make the solution to the elliptic boundary value problem from the balance of momentum have a singular solution in the sense that for dimensionality higher than one, no formal solutions in the finite-element space $\boldsymbol{H^1}$ exist. Placidi [18], Yang and Misra [23], Putar et al. [19], Andreaus et al. [1], among others, consider point forces on edges or corners using high-order gradient theories that are suitable for the incorporation of nonlinear effects from large strains. Reiher et al. [20] describe a three-dimensional finite element implementation of point forces along edges or corners that is based on a Hellinger–Reissner variational principle. The numerical simulations indicate that singularities that would be there if linear elasticity is used, could be removed by the implementation of linear second-strain gradient elasticity.

Although in classical finite-element strategies, one uses for instance piecewise linear Lagrangian elements, of which the basis functions are in $\boldsymbol{H^1}$, and therewith one attempts to approximate the solution (which is not in $\boldsymbol{H^1}$) as well as possibly by a function in $\boldsymbol{H^1}$. Bertoluzza et al. [4] demonstrated the convergence of finite-element solutions to an elliptic problem with Dirac Delta distributions by means of piecewise linear Lagrangian elements in multiple dimensions. In our earlier studies [16,17], we proved the convergence of solutions obtained by regularization of the Dirac Delta distributions, the so-called smoothed particle approach and the so-called 'hole' approach to the solution obtained by the Dirac Delta distributions in the one- and two-dimensional cases. In the one-dimensional case, for the sake of completeness, we start with the presentation of force equilibrium with point forces, the equations are given by

$$-\frac{d\sigma}{dx} = f, \qquad \text{Equation of Equilibrium,} \tag{1}$$

$$\epsilon = \frac{du}{dx}, \qquad \text{Strain–Displacement Relation,} \tag{2}$$

$$\sigma = E\epsilon, \qquad \text{Constitutive Equation.} \tag{3}$$

To simplify the equation, we use $E = 1$ here, the equations above can be combined to the one-dimensional Poisson equation:

$$-\frac{d^2u}{dx^2} = f. \tag{4}$$

We assume that there is a biological cell with size h and centre position c in the computational domain such that $0 < c - h/2 < c < c + h/2 < L$. Then the force is given by $f = \delta(x - (c - h/2)) - \delta(x - (x + h/2))$. Combined with homogeneous Dirichlet boundary conditions:

$$u(0) = 0, \;\; u(L) = 0,$$

the Galerkin form is given by

$$\begin{cases} \text{Find } u_h \in H_0^1((0,L)), \text{ such that} \\ \int_\Omega u_h' \phi_h' d\Omega = \phi_h(c - \frac{h}{2}) - \phi_h(c + \frac{h}{2}), \\ \text{for all } \phi_h \in H_0^1((0,L)). \end{cases}$$

The exact solution is

$$u(x) = \frac{hx}{L} + (x - (c + \frac{h}{2}))_+ - (x - (c - \frac{h}{2}))_+,$$

where $(x)_+ = \max\{0, x\}$. Note that in one dimension, the solution is piecewise linear and hence in $H^1(\Omega)$, however not in $H^2(\Omega)$. Since most conventional errors are expressed in the L^2-norm of the second derivative of the solution, one may not apriorily expect very accurate finite element solutions.

In the current manuscript we extend the results to general dimensionality. The boundary value problem is stated in Section 2. The 'hole' approach and the smoothed particle approach are developed in Section 3. Furthermore, we prove consistency between all the alternatives and the immersed boundary approach in multi dimensions. Section 5 displays some conclusions and discussions.

2. Elasticity equation with point sources in multi dimensions

Let Ω be a bounded domain in $\mathbb{R}^n$, then we consider the following balance of momentum where inertial effects have been neglected:

$$-\nabla \cdot \boldsymbol{\sigma} = \boldsymbol{f}. \tag{5}$$

Here $\boldsymbol{\sigma}$ denotes the stress tensor and $\boldsymbol{f}$ represents a body force that is exerted within Ω. We consider a linear, homogeneous, isotropic and continuous material; hence, Hooke's Law is used here for the relation between the stress and strain tensors:

$$\boldsymbol{\sigma} = \frac{E}{1+\nu} \left\{ \boldsymbol{\epsilon} + \text{tr}(\boldsymbol{\epsilon}) \left[\frac{\nu}{1-2\nu} \right] \boldsymbol{I} \right\}, \tag{6}$$

where E is the stiffness of the computational domain, ν is Poisson's ratio of the computational domain and $\boldsymbol{\epsilon}$ is the infinitesimal Eulerian strain tensor:

$$\boldsymbol{\epsilon} = \frac{1}{2} \left[\nabla \boldsymbol{u} + (\nabla \boldsymbol{u})^T \right]. \tag{7}$$

Within the domain of computation, Ω, we consider the presence of a biological cell, which occupies the portion Ω_C that is completely embedded within Ω (hence Ω_C is a strict subset of Ω). The boundary of the cell Γ_C is divided into surface elements. On the centre of each surface element, a point force by means of Dirac Delta distributions, is exerted in the direction of the normal vector that is directed inward into the cell. This results into (see [22]):

$$\boldsymbol{f}_t = \sum_{j=1}^{N_S} P(\boldsymbol{x}_j, t) \boldsymbol{n}(\boldsymbol{x}_j) \delta(\boldsymbol{x} - \boldsymbol{x}_j(t)) \Delta S(\boldsymbol{x}_j(t)), \tag{8}$$

where N_S is the number of surface elements of the cell, $P(\boldsymbol{x}, t)$ is the magnitude of the pulling force exerted at point $\boldsymbol{x}$ and time t per unit of measure (being area in $\mathbb{R}^3$ or length in $\mathbb{R}^2$), $\boldsymbol{n}(\boldsymbol{x})$ is the unit inward pointing normal vector (towards the cell centre) at position $\boldsymbol{x}$, $\boldsymbol{x}_j(t)$ is the midpoint on surface element j of the cell at time t and $\Delta S(\boldsymbol{x}_j)$ is the measure of the surface element j. In the general model where we use this principle, we consider transient effects due to migration and possible deformation of the cells. However, since we predominantly focus on the mathematical issues in the current manuscript, we will not consider any time-dependencies and hence t will be removed from the expressions in the remainder of the paper.

In the n-dimensional case, we are solving the boundary value problems described in Eq. (5), (6) and (7). The body force is given in Eq. (8). Therefore, the immersed boundary value problem that we are going to consider is given by

$$(BVP)\begin{cases}-\nabla\cdot\boldsymbol{\sigma}(\boldsymbol{x})=\displaystyle\sum_{j=1}^{N_S}P(\boldsymbol{x}_j)\boldsymbol{n}(\boldsymbol{x}_j)\delta(\boldsymbol{x}-\boldsymbol{x}_j)\Delta S(\boldsymbol{x}_j),\text{ in }\Omega,\\ \qquad\qquad \boldsymbol{u}=\boldsymbol{0},\text{ on }\partial\Omega.\end{cases}$$

Next to this boundary value problem, we consider the continuous immersed boundary counterpart, given by

$$(BVP_\infty)\begin{cases}-\nabla\cdot\boldsymbol{\sigma}(\boldsymbol{x})=\displaystyle\int_{\Gamma_C}P(\boldsymbol{x}')\boldsymbol{n}(\boldsymbol{x}')\delta(\boldsymbol{x}-\boldsymbol{x}')dS(\boldsymbol{x}'),\text{ in }\Omega,\\ \qquad\qquad \boldsymbol{u}=\boldsymbol{0},\text{ on }\partial\Omega,\end{cases}$$

where we take $N_s\to\infty$. Thus, the body force reads as

$$\boldsymbol{f}_t^\infty=\int_{\Gamma_C}P(\boldsymbol{x}')\boldsymbol{n}(\boldsymbol{x}')\delta(\boldsymbol{x}-\boldsymbol{x}')dS(\boldsymbol{x}'). \tag{9}$$

Due to the irregular nature of the Dirac Delta distributions, the solutions do not exist in $\boldsymbol{H^1}$, see for instance [3], where fundamental solutions for the two-dimensional linear elasticity equations are given for an unbounded domain. The idea [10] of having a particular solution in combination with a solution to the homogeneous elasticity equation with the fundamental solution as a boundary condition (singularity removal method) can be used to demonstrate this fact. We attempt to approximate the solution by the functions in $\boldsymbol{H^1}$, via the Galerkin form of (BVP) and (BVP_∞). In this manuscript, piecewise linear Lagrangian basis functions are selected and we will demonstrate convergence of the "Galerkin solutions" of (BVP) and (BVP_∞). Further, the convergence of the finite-element solutions for elliptic problems with a Dirac Delta distribution using linear Lagrangian elements in general dimensionality has been proved in [4,7,13,21].

To construct the Galerkin form, we introduce the bilinear form $a(.,.)$

$$a(\boldsymbol{u}_h,\boldsymbol{\phi}_h)=\int_\Omega\boldsymbol{\sigma}(\boldsymbol{u}_h):\nabla\boldsymbol{\phi}_h d\Omega=\int_\Omega\boldsymbol{\sigma}(\boldsymbol{u}_h):\boldsymbol{\epsilon}(\boldsymbol{\phi}_h)d\Omega, \tag{10}$$

where the last step is motivated by symmetry of the stress tensor $\boldsymbol{\sigma}$. Since the solution $\boldsymbol{u}$ is not in $\boldsymbol{H^1}(\Omega)$, we consider a subspace of $\boldsymbol{H^1}(\Omega)$, which is defined as $\boldsymbol{V_h}(\Omega)=\text{Span}\{\boldsymbol{\phi^1},\boldsymbol{\phi^2},\dots,\boldsymbol{\phi^N}\}$ [21]. Here, $\boldsymbol{\phi^i}$ for $i=\{1,2,\dots,N\}$ is the linear Lagrangian basis function, which is piecewise smooth and continuous over Ω. Hence, these basis functions are in $\boldsymbol{H^1}$. Subsequently, the Galerkin form is

$$(GF)\begin{cases}\text{Find }\boldsymbol{u}_h\in\boldsymbol{V}_h(\Omega),\text{ such that}\\ a(\boldsymbol{u}_h,\boldsymbol{\phi}_h)=(\boldsymbol{\phi}_h,\boldsymbol{f}_t)=\displaystyle\sum_{j=1}^{N_S}P(\boldsymbol{x}_j)\boldsymbol{n}(\boldsymbol{x}_j)\boldsymbol{\phi}_h(\boldsymbol{x}_j)\Delta S(\boldsymbol{x}_j),\\ \text{for all }\boldsymbol{\phi}_h\in\{\boldsymbol{\phi^1},\boldsymbol{\phi^2},\dots,\boldsymbol{\phi^N}\}\subset\boldsymbol{V}_h(\Omega).\end{cases}$$

We further consider the solution to the continuous immerse boundary problem, with the following Galerkin form:

$$(GF_\infty)\begin{cases}\text{Find }\boldsymbol{u}_h\in\boldsymbol{V}_h(\Omega),\text{ such that}\\ a(\boldsymbol{u}_h,\boldsymbol{\phi}_h)=(\boldsymbol{\phi}_h,\boldsymbol{f}_t^\infty)=\displaystyle\int_{\Gamma_C}P(\boldsymbol{x}')\boldsymbol{n}(\boldsymbol{x}')\boldsymbol{\phi}_h(\boldsymbol{x}')dS(\boldsymbol{x}'),\\ \text{for all }\boldsymbol{\phi}_h\in\{\boldsymbol{\phi^1},\boldsymbol{\phi^2},\dots,\boldsymbol{\phi^N}\}\subset\boldsymbol{V}_h(\Omega).\end{cases}$$

Before we proceed to claim the existence and the uniqueness of the Galerkin solution in (GF), we state Korn's Inequality in multiple dimensions:

Lemma 1 (*Korn's Second Inequality [6]*)**.** *Let $\Omega\subset\mathbb{R}^n$ be an open, bounded and connected domain. Then there exists a positive constant K, such that for any vector-valued function $\boldsymbol{u}\in\boldsymbol{H_0^1}(\Omega)$,*

$$\int_\Omega\|\boldsymbol{\epsilon}(\boldsymbol{u})\|^2d\Omega\geqslant K\|\boldsymbol{u}\|^2_{\boldsymbol{H^1}(\Omega)}.$$

We note that Korn's Second Inequality can be generalized to cases in which the boundary condition $\boldsymbol{u} = \boldsymbol{0}$ is imposed only on a non-zero measure part of the boundary. Using Korn's Second inequality gives the following lemma:

Lemma 2. *Let $\Omega \subset \mathbb{R}^n$ be an open, bounded and connected domain. Then there exists a positive constant K, such that for any vector-valued function $\boldsymbol{u} \in \boldsymbol{H}_{\boldsymbol{0}}^{\boldsymbol{1}}(\Omega)$,*

$$a(\boldsymbol{u}, \boldsymbol{u}) = \int_{\Omega} \boldsymbol{\sigma}(\boldsymbol{u}) : \boldsymbol{\epsilon}(\boldsymbol{u}) d\Omega \geqslant K \|\boldsymbol{u}\|^2_{\boldsymbol{H}^{\boldsymbol{1}}(\Omega)}.$$

Proof. The lemma directly follows from the definition of the stress tensor, let $\boldsymbol{u} \in \boldsymbol{H}_{\boldsymbol{0}}^{\boldsymbol{1}}(\Omega)$:

$$\begin{aligned} a(\boldsymbol{u}, \boldsymbol{u}) &= \int_{\Omega} \boldsymbol{\sigma}(\boldsymbol{u}) : \boldsymbol{\epsilon}(\boldsymbol{u}) d\Omega \\ &= \int_{\Omega} \frac{E}{1+\nu} \left\{ \boldsymbol{\epsilon}(\boldsymbol{u}) + \operatorname{tr}(\boldsymbol{\epsilon}(\boldsymbol{u})) \frac{\nu}{1-2\nu} \boldsymbol{I} \right\} : \boldsymbol{\epsilon}(\boldsymbol{u}) d\Omega \\ &= \int_{\Omega} \frac{E}{1+\nu} \|\boldsymbol{\epsilon}(\boldsymbol{u})\|^2 + \frac{E\nu}{(1+\nu)(1-2\nu)} (\operatorname{tr}(\boldsymbol{\epsilon}(\boldsymbol{u})))^2 d\Omega \\ &\geqslant \frac{E}{1+\nu} K \|\boldsymbol{u}\|^2_{\boldsymbol{H}^{\boldsymbol{1}}(\Omega)}. \end{aligned}$$

The last step follows from Lemma 1. Hence, redefining $K := \frac{E}{1+\nu} K$ concludes the proof the lemma. □

Herewith, coerciveness of the linear form $a(.,.)$ has been demonstrated, which is needed for the proof of existence and uniqueness of the Galerkin finite-element solution.

Theorem 1. *Let $\{\boldsymbol{\phi}^{\boldsymbol{i}}\}$ be piecewise Lagrangian basis field functions and let $\boldsymbol{F}$ be a vector in $\mathbb{R}^n$ with unit length, further let $P \in C(\overline{\Omega})$, and let $|P| \leqslant M_2$ for some $M_2 > 0$. We define $\boldsymbol{V}_h(\Omega) = \operatorname{Span}\{\boldsymbol{\phi}^{\boldsymbol{1}}, \boldsymbol{\phi}^{\boldsymbol{2}}, \ldots, \boldsymbol{\phi}^{N}\} \subset \boldsymbol{H}_{\boldsymbol{0}}^{\boldsymbol{1}}(\Omega)$, then*

- *$\exists\, !\; \boldsymbol{u}_h^G(\boldsymbol{x}; \boldsymbol{x}'; \boldsymbol{F}) \in \boldsymbol{V}_h(\Omega)$ such that $a(\boldsymbol{u}_h, \boldsymbol{\phi}_h) = \boldsymbol{F}(\boldsymbol{x}') \cdot \boldsymbol{\phi}_h(\boldsymbol{x}')$ for all $\boldsymbol{\phi}_h \in \boldsymbol{V}_h$;*
- *$\exists\, !\; \boldsymbol{u}_h \in \boldsymbol{V}_h(\Omega)$ such that*

  $$a(\boldsymbol{u}_h, \boldsymbol{\phi}_h) = \sum_{j=1}^{N_S} P(\boldsymbol{x}_j) \boldsymbol{n}(\boldsymbol{x}_j) \boldsymbol{\phi}_h(\boldsymbol{x}_j) \Delta S(\boldsymbol{x}_j),$$

  for all $\boldsymbol{\phi}_h \in \boldsymbol{V}_h$, and

  $$\boldsymbol{u}_h = \sum_{j=1}^{N_S} P(\mathbf{x}_j) \mathbf{u}_h^G(\mathbf{x}; \mathbf{x}_j; \mathbf{n}(\mathbf{x}_j)) \Delta S(\mathbf{x}_j);$$

- *$\exists\, !\; \boldsymbol{u}_h \in \boldsymbol{V}_h(\Omega)$ such that*

  $$a(\boldsymbol{u}_h, \boldsymbol{\phi}_h) = \int_{\Gamma_C} P(\boldsymbol{x}') \boldsymbol{n}(\boldsymbol{x}') \boldsymbol{\phi}_h(\boldsymbol{x}') dS(\boldsymbol{x}'),$$

  for all $\boldsymbol{\phi}_h \in \boldsymbol{V}_h$, and

  $$\boldsymbol{u}_h = \int_{\Gamma_C} P(\mathbf{x}') \mathbf{u}_h^G(\mathbf{x}; \mathbf{x}'; \mathbf{n}(\mathbf{x}')) dS(\boldsymbol{x}');$$

Proof.

- It is immediately clear that $a(.,.)$ is a bilinear form. We have $\boldsymbol{V}_h \subset \boldsymbol{H}_{\boldsymbol{0}}^{\boldsymbol{1}}(\Omega)$, and $a(.,.)$ is bounded in $\boldsymbol{H}_{\boldsymbol{0}}^{\boldsymbol{1}}(\Omega)$ (see for instance [2]). Furthermore, Lemma 2 says that $a(.,.)$ is coercive in $\boldsymbol{H}_0^1(\Omega)$. Regarding the right-hand side, we have $|\boldsymbol{\phi}_h| \leq M_1$ for some $M_1 > 0$ since $\boldsymbol{\phi}_h$ is a Lagrangian function, and hence the magnitude of the right-hand side can be bounded from above by

$$|\boldsymbol{F} \cdot \boldsymbol{\phi}_h(\boldsymbol{x}')| \leqslant M_1.$$

Note that $\|\boldsymbol{F}\| = 1$. Hence the right-hand side is bounded, since we are looking for a solution in a finite dimensional space $\boldsymbol{V}_h$, the system

$$A\boldsymbol{c} = \boldsymbol{b},$$

where the coefficients of the symmetric matrix A are defined by $a_{ij} = a(\phi_i, \phi_j)$, and where a limited number of entries of $\boldsymbol{b}$ are non-zero and given by $\boldsymbol{F} \cdot \boldsymbol{\phi}_h(\boldsymbol{x}')$, which is finite. Since $\boldsymbol{b}$ is finite, and A is invertible, existence and uniqueness of $\boldsymbol{u}_h$ follow (one could apply Lax–Milgram's theorem on the space $\mathbb{R}^n$ in this context) from the algebraic system.

- Existence and uniqueness follow analogously, only boundedness of the right-hand side, which is a linear functional in $\boldsymbol{\phi}_h \in \boldsymbol{V}_h(\Omega)$ has to be checked:

$$\begin{aligned}
&\left|\sum_{j=1}^{N_S} P(\boldsymbol{x}_j)\boldsymbol{n}(\boldsymbol{x}_j) \cdot \boldsymbol{\phi}_h(\boldsymbol{x}_j)\Delta S(\boldsymbol{x}_j)\right| \\
&\leqslant \sum_{j=1}^{N_S} |P(\boldsymbol{x}_j)|\|\boldsymbol{n}(\boldsymbol{x}_j)\|\|\boldsymbol{\phi}_h(\boldsymbol{x}_j)\|\Delta S(\boldsymbol{x}_j) \\
&= \sum_{j=1}^{N_S} |P(\boldsymbol{x}_j)|\|\boldsymbol{\phi}_h(\boldsymbol{x}_j)\|\Delta S(\boldsymbol{x}_j) \leqslant M_1 M_2 \sum_{j=1}^{N_S} \Delta S(\boldsymbol{x}_j).
\end{aligned}$$

Note that $\boldsymbol{n}$ has unit length. The summation gives the polygonal length or polyhedral area of the cell boundary. Hence the right-hand side is bounded, then by Lax–Milgram's Lemma, existence and uniqueness follow. Further by substitution, it follows that

$$\begin{aligned}
a(\boldsymbol{u}_h, \boldsymbol{\phi}_h) &= a(\sum_{j=1}^{N_S} P(\boldsymbol{x}_j)\boldsymbol{u}_h^G(\boldsymbol{x}, \boldsymbol{x}_j, \boldsymbol{n}(\boldsymbol{x}_j))\Delta S(\boldsymbol{x}_j), \boldsymbol{\phi}_h) \\
&= \sum_{j=1}^{N_S} P(\boldsymbol{x}_j) a(\boldsymbol{u}_h^G(\boldsymbol{x}, \boldsymbol{x}_j, \boldsymbol{n}(\boldsymbol{x}_j)), \boldsymbol{\phi}_h)\Delta S(\boldsymbol{x}_j) \\
&= \sum_{j=1}^{N_S} P(\boldsymbol{x}_j)\boldsymbol{n}(\boldsymbol{x}_j) \cdot \boldsymbol{\phi}_h(\boldsymbol{x}_j)\Delta S(\boldsymbol{x}_j).
\end{aligned}$$

The last step uses the first part of the theorem, and finally the assertion is proved similarly to the first assertion.

- We proceed similarly, by boundedness of the right-hand side:

$$\left|\int_{\Gamma_C} P(\boldsymbol{x}')\boldsymbol{n}(\boldsymbol{x}') \cdot \boldsymbol{\phi}_h(\boldsymbol{x}') dS(\boldsymbol{x}')\right| \leqslant M_1 M_2 |\Gamma_C|,$$

where $|\Gamma_C|$ is the measure of the boundary surface of the biological cell. It again shows that the right-hand side is a bounded linear functional in $\boldsymbol{V}_h(\Omega)$. We proceed by substitution:

$$\begin{aligned}
a(\boldsymbol{u}_h, \boldsymbol{\phi}_h) &= a(\int_{\Gamma_C} P(\boldsymbol{x}')\boldsymbol{u}_h^G(\boldsymbol{x}, \boldsymbol{x}', \boldsymbol{n}(\boldsymbol{x}')) dS(\boldsymbol{x}'), \boldsymbol{\phi}_h) \\
&= \int_{\Gamma_C} P(\boldsymbol{x}') a(\boldsymbol{u}_h^G(\boldsymbol{x}, \boldsymbol{x}', \boldsymbol{n}(\boldsymbol{x}')), \boldsymbol{\phi}_h) dS(\boldsymbol{x}') \\
&= \int_{\Gamma_C} P(\boldsymbol{x}')\boldsymbol{n}(\boldsymbol{x}') \cdot \boldsymbol{\phi}_h(\boldsymbol{x}') dS(\boldsymbol{x}').
\end{aligned}$$

Note that, formally, it was not necessary to prove boundedness, since coerciveness implies uniqueness and the existence was proved by construction and by combining the result for the existence of $\boldsymbol{u}_h^G$. □

Note that for the ‘continuous’ weak formulation, there is no solution in $\boldsymbol{H}^1$, hence the above claim demonstrates the existence and uniqueness of a Galerkin-based approximation in a subset of $\boldsymbol{H}^1$ to a function that is not in $\boldsymbol{H}^1$. The situation is somewhat comparable to approximating $\sqrt{2} \notin \mathbb{Q}$ arbitrarily accurately by a sequence of successive approximations in $\mathbb{Q}$. Further in two- and three-dimensional case, the convergence between the solution to (GF) and (GF_∞) can be proved. Similar work has been done in [14] regarding Stokes problem with the Delta distribution term.

Theorem 2. *Let Γ_C be a polygon or polyhedron embedded in $\Omega \subset \mathbb{R}^n$ and let $P(\boldsymbol{x})$ be sufficiently smooth. Further, let $\boldsymbol{x}_j$ be the midpoint of surface element $\Delta S(\boldsymbol{x}_j)$. Denote $\boldsymbol{u}_h^{\Delta S}$ as the Galerkin solution to (GF) and the $\boldsymbol{u}_h^{\infty}$ as the Galerkin solution to (GF_∞), respectively. In two dimensions, for any $\boldsymbol{x} \notin \Gamma_C$, there exists a positive constant C, such that for each component of $\boldsymbol{u}_h^{\infty}$ we have*

$$|\boldsymbol{u}_h^{\Delta S} - \boldsymbol{u}_h^{\infty}| \leqslant C \Delta S_{max}^2,$$

where $\Delta S_{max} = \max\{\Delta S(\boldsymbol{x}_j)\}$ for any $j = \{1, 2, \ldots, N_S\}$. In three dimensions, for any $\boldsymbol{x} \notin \Gamma_C$, there exists a positive constant C, such that for each component of $\boldsymbol{u}_h^{\infty}$ we have

$$|\boldsymbol{u}_h^{\Delta S} - \boldsymbol{u}_h^{\infty}| \leqslant C h_{max}^2,$$

where h_{max} is the maximal diameter among all the triangular elements over Γ_C.

Proof. Away from Γ_C, the function $\boldsymbol{u}_h^G$ is smooth, and since $P(\boldsymbol{x})$ is smooth as well, the integrand, given by $P(\boldsymbol{x})\boldsymbol{u}_h^G$ is smooth as well. For ease of notation, we set $\boldsymbol{f}(\boldsymbol{x}) = P(\boldsymbol{x})\boldsymbol{u}_h^G(\boldsymbol{x}; \boldsymbol{x}'; \boldsymbol{n})$. We start with the 2D-case. Given the ith boundary element ΔS_i on Γ_C with the endpoints $\boldsymbol{x}_i$ and $\boldsymbol{x}_{i+1}$ and we denote its midpoint by $\boldsymbol{x}_{i+1/2}$, where $i \in \{1, 2, \ldots, N_S\}$. We consider

$$\boldsymbol{x}(s) = \boldsymbol{x}_{i+1/2} + s\frac{\boldsymbol{x}_{i+1} - \boldsymbol{x}_i}{2}, \quad -1 \leqslant s \leqslant 1.$$

Hence, $\boldsymbol{x}(0) = \boldsymbol{x}_{i+1/2}$ and $\boldsymbol{x}'(s) = \frac{1}{2}(\boldsymbol{x}_{i+1} - \boldsymbol{x}_1)$, and subsequently

$$\|\boldsymbol{x}'(s)\| = \frac{1}{2}\|\boldsymbol{x}_{i+1} - \boldsymbol{x}_1\|.$$

We calculate the contribution over ΔS_i to the integral, where Taylor’s Theorem and the Mean Value Theorem for integration are used to warrant the existence of a $\hat{s} \in (-1, 1)$, such that

$$\begin{aligned}
&\int_{\Delta S_i} \boldsymbol{f}(\boldsymbol{x}) dS = \int_{-1}^{1} \boldsymbol{f}(\boldsymbol{x}(s))\|\boldsymbol{x}'(s)\| ds \\
&= \frac{1}{2}\|\boldsymbol{x}_{i+1} - \boldsymbol{x}_i\| \int_{-1}^{1} \boldsymbol{f}(\boldsymbol{x}(s)) ds \\
&\text{(Taylor Expansion)} = \frac{1}{2}\|\boldsymbol{x}_{i+1} - \boldsymbol{x}_i\| \int_{-1}^{1} \boldsymbol{f}(\boldsymbol{x}(0)) + s\frac{\boldsymbol{x}_{i+1} - \boldsymbol{x}_i}{2}\nabla \boldsymbol{f}(\boldsymbol{x}(s))|_{s=0} \\
&+ \frac{1}{2}s^2(\frac{\boldsymbol{x}_{i+1} - \boldsymbol{x}_i}{2})^T \boldsymbol{H}(\boldsymbol{x}(\hat{s}))(\frac{\boldsymbol{x}_{i+1} - \boldsymbol{x}_i}{2}) ds \\
&= \frac{1}{2}\|\boldsymbol{x}_{i+1} - \boldsymbol{x}_i\|[2\boldsymbol{f}(\boldsymbol{x}_{i+1/2}) + 0 + \frac{1}{12}(\boldsymbol{x}_{i+1} - \boldsymbol{x}_i)^T \boldsymbol{H}(\boldsymbol{x}(\hat{s}))(\boldsymbol{x}_{i+1} - \boldsymbol{x}_i)] \\
&= \|\boldsymbol{x}_{i+1} - \boldsymbol{x}_i\|\boldsymbol{f}(\boldsymbol{x}_{i+1/2}) + \frac{1}{24}\|\boldsymbol{x}_{i+1} - \boldsymbol{x}_i\|(\boldsymbol{x}_{i+1} - \boldsymbol{x}_i)^T \boldsymbol{H}(\boldsymbol{x}(\hat{s}))(\boldsymbol{x}_{i+1} - \boldsymbol{x}_i),
\end{aligned}$$

where $\boldsymbol{H}(\boldsymbol{x}(s))$ is the Hessian matrix of $f(\boldsymbol{x}(s))$. Therefore, we obtain that

$$\begin{aligned}
&\left|\int_{\Delta S_i} \boldsymbol{f}(\boldsymbol{x}) dS - \|\boldsymbol{x}_{i+1} - \boldsymbol{x}_1\|\boldsymbol{f}(\boldsymbol{x}_{i+1/2})\right| \\
&= \frac{1}{24}\|\boldsymbol{x}_{i+1} - \boldsymbol{x}_i\| \cdot |(\boldsymbol{x}_{i+1} - \boldsymbol{x}_i)^T \boldsymbol{H}(\boldsymbol{x}(\hat{s}))(\boldsymbol{x}_{i+1} - \boldsymbol{x}_i)| \\
&\leqslant \frac{1}{24}\|\boldsymbol{x}_{i+1} - \boldsymbol{x}_i\|\tilde{K}\|\boldsymbol{x}_{i+1} - \boldsymbol{x}_i\|^2.
\end{aligned}$$

Since $\boldsymbol{f}(\boldsymbol{x}) \in \boldsymbol{C}^2(\Omega)$, it follows that there exists a $\tilde{K} > 0$, such that

$$|(\boldsymbol{x}, \boldsymbol{H}(\boldsymbol{x}))| \leqslant \tilde{K}\|\boldsymbol{x}\|^2.$$

Therefore, considering the summation of the boundary elements over $\partial\Omega_C$,

$$\begin{aligned}\left|\int_{\Delta S_i} \boldsymbol{f}(\boldsymbol{x})dS - \sum_{i=1}^{N_S}\|\boldsymbol{x}_{i+1}-\boldsymbol{x}_1\|\boldsymbol{f}(\boldsymbol{x}_{i+1/2})\right| &\leqslant \sum_{i=1}^{N_S}\frac{1}{24}\|\boldsymbol{x}_{i+1}-\boldsymbol{x}_i\|\tilde{K}\|\boldsymbol{x}_{i+1}-\boldsymbol{x}_i\|^2 \\ &\leqslant \frac{1}{24}\tilde{K}\Delta S_{max}^2\sum_{i=1}^{N_S}\|\boldsymbol{x}_{i+1}-\boldsymbol{x}_i\| \\ &= \frac{1}{24}\tilde{K}\Delta S_{max}^2|\Gamma_C|,\end{aligned}$$

where $\Delta S_{max} = \max_{i\in\{1,\dots,N_S\}}\|\boldsymbol{x}_{i+1}-\boldsymbol{x}_i\|$ is the maximal length of the line segment over Γ_C, and $|\Gamma_C|$ is the perimeter of the polygon Γ_C. It can be concluded that there exists a positive constant K, such that

$$|\boldsymbol{u}_h^{\infty} - \boldsymbol{u}_h^{\Delta S}| \leqslant K\Delta S_{max}^2.$$

In three dimensions, the surface element over a manifold is a triangle. We map the triangle in (x, y, z)-space to the reference triangle in (s, t)-space with points $(0, 0), (0, 1)$ and $(1, 0)$. Suppose there is a surface element e_j with nodal points $\boldsymbol{x}_1, \boldsymbol{x}_2$ and $\boldsymbol{x}_3$, then the centre point of e_j is $\boldsymbol{x}_c = (\boldsymbol{x}_1+\boldsymbol{x}_2+\boldsymbol{x}_3)/3$. The map from the reference triangle e_0 to the physical triangle e_j is given by

$$\boldsymbol{x}(s, t) = \boldsymbol{x}_1(1-s-t) + s\boldsymbol{x}_2 + t\boldsymbol{x}_3, \quad 0 \leqslant s \leqslant 1, t \leqslant 1-s.$$

For any function $\boldsymbol{f}(\boldsymbol{x}) \in C^2(\Omega)$, the integral over the original triangle is given by

$$\int_{e_j}\boldsymbol{f}(\boldsymbol{x})d\boldsymbol{x} = \int_{e_0}\boldsymbol{f}(\boldsymbol{x}(s,t))\sqrt{\left|\det(\boldsymbol{J}^T\boldsymbol{J})\right|}d(s,t),$$

where $\boldsymbol{J}$ is the Jacobian matrix, and $e_0 = \{(s, t) \in \mathbb{R}^2 : 0 \leqslant s \leqslant 1, 0 \leqslant t \leqslant 1-s\}$ given by

$$\boldsymbol{J} = \frac{\partial(x, y, z)}{\partial(s, t)} = \begin{pmatrix} x_2 - x_1 & x_3 - x_1 \\ y_2 - y_1 & y_3 - y_1 \\ z_2 - z_1 & z_3 - z_1 \end{pmatrix},$$

and $\sqrt{|\det(\boldsymbol{J}^T\boldsymbol{J})|}$ is twice the area of the original triangle e_j, i.e.

$$|\Delta_j| := \sqrt{|\det(\boldsymbol{J}^T\boldsymbol{J})|} = \|(\boldsymbol{x}_2-\boldsymbol{x}_1)\times(\boldsymbol{x}_3-\boldsymbol{x}_1)\|.$$

We conduct the same process as for the two dimensional case, we obtain, where $\boldsymbol{x}(\frac{1}{3}, \frac{1}{3}) = \boldsymbol{x}_c$ coincides with the midpoint of element e_j, and where Taylor's Theorem for multi-variate functions is used:

$$\begin{aligned}&\int_{e_j}\boldsymbol{f}(\boldsymbol{x})d\boldsymbol{x} = \int_{e_0}\boldsymbol{f}(\boldsymbol{x}(s,t))|\Delta_j|d(s,t) \\ &= |\Delta_j|\int_{e_0}\boldsymbol{f}(\boldsymbol{x}(s,t))d(s,t) \\ &= |\Delta_j|\int_{e_0}\boldsymbol{f}(\boldsymbol{x}_c) + (\boldsymbol{x}(s,t)-\boldsymbol{x}_c)\cdot\nabla\boldsymbol{f}(\boldsymbol{x}_c) \\ &+\ \frac{1}{2}(\boldsymbol{x}(s,t)-\boldsymbol{x}_c)^T\boldsymbol{H}(\boldsymbol{x}(\hat{s},\hat{t}))(\boldsymbol{x}(s,t)-\boldsymbol{x}_c)d(s,t) \\ &= |\Delta_j|\left[\frac{1}{2}\boldsymbol{f}(\boldsymbol{x}_c) + 0\right. \\ &\left.+\frac{1}{2}\int_{e_0}(\boldsymbol{x}(s,t)-\boldsymbol{x}_c)^T\boldsymbol{H}(\boldsymbol{x}(\hat{s},\hat{t}))(\boldsymbol{x}(s,t)-\boldsymbol{x}_c)d(s,t)\right].\end{aligned}$$

Due to $\boldsymbol{f}(\boldsymbol{x}) \in \boldsymbol{C}^2(\Omega)$, then for the Hessian matrix of $\boldsymbol{f}(\boldsymbol{x})$, there exists $\tilde{K} > 0$, such that

$$|(\boldsymbol{x}, \boldsymbol{H}(\boldsymbol{x}))| \leqslant \tilde{K}\|\boldsymbol{x}\|^2.$$

It yields

$$\begin{aligned}
&\left|\int_{e_j} \boldsymbol{f}(\boldsymbol{x})d\boldsymbol{x} - \frac{|\Delta_j|}{2}\boldsymbol{f}(\boldsymbol{x}_c)\right| \\
&\leqslant \left|\frac{|\Delta_j|}{2}\int_{e_0} (\boldsymbol{x}(s,t) - \boldsymbol{x}_c)^T \boldsymbol{H}(\boldsymbol{x}(\hat{s},\hat{t}))(\boldsymbol{x}(s,t) - \boldsymbol{x}_c)d(s,t)\right| \\
&\leqslant \frac{|\Delta_j|}{4}\tilde{K}h_{max}^2,
\end{aligned}$$

where h_{max}^2 is the largest diameter in the original triangle e_j. Considering all the surface elements over Γ_C, we compute

$$\left|\int_{\Gamma_C} \boldsymbol{f}(\boldsymbol{x})d\boldsymbol{x} - \sum_{j=1}^{N_S}\frac{|\Delta_j|}{2}\boldsymbol{f}(\boldsymbol{x}_j)\right| \leqslant \frac{\tilde{K}}{4}h_{max}^2\sum_{j=1}^{N_S}\frac{|\Delta_j|}{2} = \frac{\tilde{K}}{4}h_{max}^2|\Gamma_C|,$$

where h_{max}^2 is the maximal diameter among all the surface element (i.e. triangle) and $|\Gamma_C|$ is the sum of the measures (area in $\mathbb{R}^3$) of all the surface elements over Γ_C. Therefore, in three dimensions, we can conclude that there exists a positive constant K, such that for the unique Galerkin solution to both (GF) and (GF_∞),

$$\left|\boldsymbol{u}_h^\infty - \boldsymbol{u}_h^{\Delta S}\right| \leqslant Kh_{max}^2. \quad \square$$

The above proof and theorem can easily be extended to higher dimensionalities.

3. Alternative approaches for elasticity equation with point sources in multi dimensions

3.1. The 'hole' approach

A different approach is based on considering cellular forces on the cell boundary by means of a boundary condition. In this alternative approach, one 'removes' the cell region from the domain of computation. Herewith, one creates a 'hole' in the domain. We consider the balance of momentum over $\Omega \setminus \overline{\Omega}_C$. This gives the following boundary value problem:

$$(BVP_H)\begin{cases} -\nabla\cdot\boldsymbol{\sigma} = 0, & \text{in } \Omega\setminus\overline{\Omega}_C, \\ \boldsymbol{\sigma}\cdot\boldsymbol{n} = P(\boldsymbol{x})\boldsymbol{n}(\boldsymbol{x}), & \text{on } \partial\Omega_C, \\ \boldsymbol{u} = \boldsymbol{0}, & \text{on } \partial\Omega, \end{cases}$$

where $\boldsymbol{\sigma}$ is defined in Eq. (6) with stiffness E. Let $D \subset \Omega$, then we introduce the following notation:

$$a_{D,E}(\boldsymbol{u},\boldsymbol{v}) := \int_D \boldsymbol{\sigma}(\boldsymbol{u}) : \boldsymbol{\epsilon}(\boldsymbol{v})d\Omega.$$

Note that the stiffness can be a constant or a function of space over the domain D.

The corresponding weak form is stated below:

$$(WF_H)\begin{cases} \text{Find } \boldsymbol{u}^H \in \boldsymbol{H}^1(\Omega\setminus\Omega_C) \text{ such that} \\ a_{\Omega\setminus\Omega_C,E}(\boldsymbol{u}^H,\boldsymbol{\phi}) = \displaystyle\int_{\Gamma_C} P(\boldsymbol{x})\boldsymbol{n}(\boldsymbol{x})\cdot\boldsymbol{\phi}dS(\boldsymbol{x}), \\ \text{for all } \boldsymbol{\phi} \in \boldsymbol{H}^1(\Omega\setminus\Omega_C). \end{cases}$$

Since $\boldsymbol{\phi} \in \boldsymbol{H}^1(\Omega\setminus\Omega_C)$, it follows from the Trace Theorem [6], and by noting that $\boldsymbol{\phi}|_{\partial\Omega} = 0$, that there is a $C_1 > 0$ such that $\|\boldsymbol{\phi}\|_{\boldsymbol{L}^2(\Gamma_C)} \leq C_1\|\boldsymbol{\phi}\|_{\boldsymbol{H}^1(\Omega)}$, which implies that the right-hand side in the weak form is bounded. Subsequently one combines Korn's Inequality with Lax–Milgram's Lemma to conclude that a unique solution in $\boldsymbol{H}^1$ exists.

We compare the immersed boundary method with the ‘hole’ approach by taking $\beta \geqslant 0$, then we adjust the immersed boundary method such that

$$E(\boldsymbol{x}) = \begin{cases} \beta E, & \text{in } \Omega_C, \\ E, & \text{in } \Omega \setminus \overline{\Omega}_C. \end{cases} \tag{11}$$

Regarding the adjusted immersed boundary approach where the stiffness is given by Eq. (11), we have the following Galerkin form

$$(GF_\beta) \begin{cases} \text{Find } \boldsymbol{u}_h^\beta \in \boldsymbol{V}_h(\Omega) \text{ such that} \\ \beta a_{\Omega_C,E}(\boldsymbol{u}_h^\beta, \boldsymbol{\phi}_h) + a_{\Omega\setminus\Omega_C,E}(\boldsymbol{u}_h^\beta, \boldsymbol{\phi}_h) = \int_{\Gamma_C} P(\boldsymbol{x})\boldsymbol{n}(\boldsymbol{x}) \cdot \boldsymbol{\phi}_h(\boldsymbol{x}) dS(\boldsymbol{x}), \\ \text{for all } \boldsymbol{\phi}_h \in \boldsymbol{V}_h(\Omega), \end{cases}$$

where $\boldsymbol{V}_h(\Omega)$ is defined in Theorem 1 in Section 2.

For the ‘hole’ approach, we have the following Galerkin form

$$(GF_H) \begin{cases} \text{Find } \boldsymbol{u}_h^H \in \boldsymbol{V}_h(\Omega \setminus \Omega_C) \text{ such that} \\ a_{\Omega\setminus\Omega_C,E}(\boldsymbol{u}_h^H, \boldsymbol{\phi}_h) = \int_{\Gamma_C} P(\boldsymbol{x})\boldsymbol{n}(\boldsymbol{x}) \cdot \boldsymbol{\phi}_h dS(\boldsymbol{x}), \\ \text{for all } \boldsymbol{\phi}_h \in \boldsymbol{V}_h(\Omega \setminus \Omega_C). \end{cases}$$

We will prove that the adjusted immersed boundary method is a perturbation of the ‘hole’ approach:

Proposition 1. *Let $\boldsymbol{u}_h^H$ and $\boldsymbol{u}_h^\beta$, respectively, satisfy Galerkin forms (GF_H) and (GF_β), then there is a $C > 0$ such that*

$$\|\boldsymbol{u}_h^H - \boldsymbol{u}_h^\beta\|_{\boldsymbol{H}^1(\Omega\setminus\Omega_C)} \leqslant C\sqrt{\beta}\|\boldsymbol{u}_h^\beta\|_{\boldsymbol{H}^1(\Omega_C)}^{1/2}.$$

Proof. First we note that, as in the spirit of Theorem 1, we consider Galerkin solutions in a subset of $\boldsymbol{H}^1$ whereas the solution to the ‘continuous’ weak formulation is not in $\boldsymbol{H}^1$. Formally (GF_H) and (GF_β) hold for test functions $\boldsymbol{\phi}_h$ from different sets, namely $\boldsymbol{V}_h(\Omega)$ and $\boldsymbol{V}_h(\Omega \setminus \Omega_C)$. If we choose $\boldsymbol{V}_h(\Omega_C)$ to correspond to Lagrangian basis functions associated to internal nodes in Ω_C, then these basis functions vanish at Γ_C. Furthermore, within the set of Lagrangian basis functions that are associated with $\Omega \setminus \Omega_C$, there are Lagrangian basis functions associated with Γ_C, which have a compact, hence limited, support over Ω_C and in $\Omega \setminus \Omega_C$, then let $\boldsymbol{v} = \boldsymbol{u}_h^\beta - \boldsymbol{u}_h^H$, then subtraction of problems (GF_H) and (GF_β) gives

$$a_{\Omega\setminus\Omega_C,E}(\boldsymbol{v}, \boldsymbol{\phi}_h) = -\beta a_{\Omega_C,E}(\boldsymbol{u}_h^\beta, \boldsymbol{\phi}_h).$$

The left-hand side is a bounded and coercive form on which we can apply Korn’s Inequality. Furthermore, boundedness of the right-hand side in $\boldsymbol{V}_h(\Omega \setminus \Omega_C)$ follows by application of the Cauchy–Schwarz Inequality, hence there is an $L > 0$ such that $|a_{\Omega_C,E}(\boldsymbol{u}_h^\beta, \boldsymbol{\phi}_h)| \leqslant L\|\boldsymbol{u}_h^\beta\|_{\boldsymbol{H}^1(\Omega_C)}\|\boldsymbol{\phi}_h\|_{\boldsymbol{H}^1(\Omega_C)}$. Herewith, we arrive at

$$-\beta L\|\boldsymbol{u}_h^\beta\|_{\boldsymbol{H}^1(\Omega_C)}\|\boldsymbol{\phi}_h\|_{\boldsymbol{H}^1(\Omega_C)} \leqslant a_{\Omega\setminus\Omega_C,E}(\boldsymbol{v}, \boldsymbol{\phi}_h) \leqslant \beta L\|\boldsymbol{u}_h^\beta\|_{\boldsymbol{H}^1(\Omega_C)}\|\boldsymbol{\phi}_h\|_{\boldsymbol{H}^1(\Omega_C)},$$
$$\text{for all } \boldsymbol{\phi}_h \in \boldsymbol{V}_h(\Omega \setminus \Omega_C).$$

Note that the $a_{\Omega\setminus\Omega_C}(\boldsymbol{v}, \boldsymbol{\phi}_h)$ contains $\boldsymbol{v}$ and $\boldsymbol{\phi}_h$ in $\Omega \setminus \Omega_C$, whereas the right-hand side of the inequality contains norms over Ω_C. Using Korn’s Inequality, and upon setting $\boldsymbol{\phi}_h = \boldsymbol{v}$ in $\Omega \setminus \Omega_C$, we arrive at

$$K\|\boldsymbol{v}\|_{\boldsymbol{H}^1(\Omega\setminus\Omega_C)}^2 \leqslant a_{\Omega\setminus\Omega_C,E}(\boldsymbol{v}, \boldsymbol{v}) \leqslant \beta L\|\boldsymbol{u}_h^\beta\|_{\boldsymbol{H}^1(\Omega_C)}\|\boldsymbol{\phi}_h\|_{\boldsymbol{H}^1(\Omega_C)}$$
$$\Rightarrow \|\boldsymbol{v}\|_{\boldsymbol{H}^1(\Omega\setminus\Omega_C)} \leqslant C\sqrt{\beta}\|\boldsymbol{u}_h^\beta\|_{\boldsymbol{H}^1(\Omega_C)}^{1/2}, \text{ where } C = \sqrt{\frac{L}{K}}\|\boldsymbol{\phi}_h\|_{\boldsymbol{H}^1(\Omega_C)}^{1/2}. \quad \square$$

For the case of a spring-force boundary condition on $\partial\Omega$ one can derive a compatibility condition. To this extent, we consider the following boundary value problems, for the 'hole' problem:

$$(BVP'_H)\begin{cases} -\nabla\cdot\boldsymbol{\sigma} = 0, & \text{in } \Omega\backslash\overline{\Omega}_C, \\ \boldsymbol{\sigma}\cdot\boldsymbol{n} = P(\boldsymbol{x})\boldsymbol{n}(\boldsymbol{x}), & \text{on } \partial\Omega_C, \\ \boldsymbol{\sigma}\cdot\boldsymbol{n} + \kappa\boldsymbol{u} = \boldsymbol{0}, & \text{on } \partial\Omega, \end{cases}$$

and for the immersed boundary problem:

$$(BVP'_I)\begin{cases} -\nabla\cdot\boldsymbol{\sigma} = \int_{\Gamma_C} P(\boldsymbol{x}')\boldsymbol{n}(\boldsymbol{x}')\delta(\boldsymbol{x}-\boldsymbol{x}')dS(\boldsymbol{x}), \text{ in } \Omega, \\ \boldsymbol{\sigma}\cdot\boldsymbol{n} + \kappa\boldsymbol{u} = \boldsymbol{0}, \text{ on } \partial\Omega, \end{cases}$$

Next we give a proposition regarding compatibility for the 'hole' approach and the immersed boundary method for the case of a spring boundary condition:

Proposition 2. *Let $\boldsymbol{u}_H$ and $\boldsymbol{u}_I$, respectively, be solutions to the 'hole' approach, see (BVP'_H) and to the immersed boundary approach, see (BVP'_I). Let Γ_C denote the boundary of the cell, over which internal forces are exerted, and let $\partial\Omega$ be the outer boundary of Ω. Then*

$$\int_{\partial\Omega}\kappa\boldsymbol{u}_H dS = \int_{\partial\Omega}\kappa\boldsymbol{u}_I dS = \int_{\Gamma_C} P(\boldsymbol{x})\boldsymbol{n}(\boldsymbol{x})dS.$$

Proof. To prove that the above equation holds true, we integrate the partial differential equation (PDE) of both approaches over the computational domain Ω.

For the immersed boundary approach, we get

$$-\int_{\Omega}\nabla\cdot\boldsymbol{\sigma}d\Omega = \int_{\Omega}\sum_{j=1}^{N_S} P(\boldsymbol{x}_j)\boldsymbol{n}(\boldsymbol{x}_j)\delta(\boldsymbol{x}-\boldsymbol{x}_j)\Delta S(\boldsymbol{x}_j)d\Omega,$$

then after applying Gauss Theorem on the left-hand side (LHS) and simplifying the right-hand side (RHS), we obtain

$$-\int_{\partial\Omega}\boldsymbol{\sigma}\cdot\boldsymbol{n}(\boldsymbol{x})dS = \sum_{j=1}^{N_S} P(\boldsymbol{x}_j)\boldsymbol{n}(\boldsymbol{x}_j)\Delta S(\boldsymbol{x}_j).$$

By substituting the Robin's boundary condition and letting $N_S \to \infty$, i.e. $\Delta S(\boldsymbol{x}_j) \to 0$, the equation becomes

$$\int_{\partial\Omega}\kappa\boldsymbol{u_I}dS = \int_{\Gamma_C} P(\boldsymbol{x})\boldsymbol{n}(\boldsymbol{x})dS. \tag{12}$$

Subsequently, we do the same thing for the 'hole' approach. Then, we get

$$-\int_{\Omega}\nabla\cdot\boldsymbol{\sigma}d\Omega = 0,$$

and we apply Gauss Theorem:

$$-\int_{\partial\Omega\cup\Gamma_C}\boldsymbol{\sigma}\cdot\boldsymbol{n}(\boldsymbol{x})dS = 0,$$

which implies

$$-\int_{\partial\Omega}\boldsymbol{\sigma}\cdot\boldsymbol{n}(\boldsymbol{x})dS - \int_{\Gamma_C}\boldsymbol{\sigma}\cdot\boldsymbol{n}(\boldsymbol{x})dS = 0.$$

Using the boundary conditions, we get

$$\int_{\partial\Omega}\kappa\boldsymbol{u}_H dS = \int_{\Gamma_C} P(\boldsymbol{x})\boldsymbol{n}(\boldsymbol{x})dS,$$

which is exactly the same as Eq. (12). Hence we proved that

$$\int_{\partial\Omega} \kappa \boldsymbol{u}_H dS = \int_{\partial\Omega} \kappa \boldsymbol{u}_I dS = \int_{\Gamma_C} P(\boldsymbol{x})\boldsymbol{n}(\boldsymbol{x}) dS. \quad \square$$

Hence, the two different approaches are consistent in the sense of global conservation of momentum and therefore the results from both approaches should be comparable.

3.2. The smoothed particle approach

The Gaussian distribution is used here as an approximation for the Dirac Delta distribution. Hereby, we show that in the n-dimensional case, the Gaussian distribution is a proper approximation for the Dirac Delta distribution.

Lemma 3. *For an open domain*

$$\Omega = (x_{1,1}, x_{1,2}) \times (x_{2,1}, x_{2,2}) \times \cdots \times (x_{n,1}, x_{n,2}) \subset \mathbb{R}^n, n \geqslant 2,$$

let

$$\delta_\varepsilon(\boldsymbol{x} - \boldsymbol{x}') = \frac{1}{(2\pi\varepsilon^2)^{n/2}} \exp\left\{-\frac{\|\boldsymbol{x} - \boldsymbol{x}'\|^2}{2\varepsilon^2}\right\},$$

where $\boldsymbol{x}' = (x_1', \ldots, x_n') \in \Omega$, *then*

(i) $\lim_{\varepsilon\to 0^+} \delta_\varepsilon(\boldsymbol{x} - \boldsymbol{x}') \to 0$, *for all* $\boldsymbol{x} \neq \boldsymbol{x}'$;

(ii) Let $f(\boldsymbol{x}) \in \mathbb{C}^2(\mathbb{R}^d)$ *and* $\|f(\boldsymbol{x})\| \leqslant M < +\infty$, *then there is a* $C > 0$ *such that*

$$\left| \int_\Omega \delta_\varepsilon(\boldsymbol{x} - \boldsymbol{x}') f(\boldsymbol{x}) d\Omega - f(\boldsymbol{x}') \right| \leqslant C\varepsilon^2 \text{ as } \varepsilon \to 0^+.$$

Proof. (i) Since $\boldsymbol{x} \neq \boldsymbol{x}'$, $\lim_{\varepsilon\to 0^+} \exp\left\{-\frac{\|\boldsymbol{x}-\boldsymbol{x}'\|^2}{2\varepsilon^2}\right\} \to 0$. Thus,

$$\lim_{\varepsilon\to 0^+} \delta_\varepsilon(\boldsymbol{x} - \boldsymbol{x}') \to 0, \text{ for all } \boldsymbol{x} \neq \boldsymbol{x}'.$$

(ii) Now we consider

$$\begin{aligned}
&\int_\Omega \delta_\varepsilon(\boldsymbol{x} - \boldsymbol{x}') f(\boldsymbol{x}) d\Omega \\
&= \int_\Omega \frac{1}{(2\pi\varepsilon^2)^{n/2}} \exp\left\{-\frac{\|\boldsymbol{x} - \boldsymbol{x}'\|^2}{2\varepsilon^2}\right\} f(\boldsymbol{x}) d\Omega.
\end{aligned}$$

Firstly, we integrate over the infinite domain:

$$\begin{aligned}
&\int_{\mathbb{R}^n} \delta_\varepsilon(\boldsymbol{x} - \boldsymbol{x}') f(\boldsymbol{x}) d\Omega \\
&= \frac{1}{(2\pi\varepsilon^2)^{n/2}} \int_{-\infty}^{+\infty} \cdots \int_{-\infty}^{+\infty} \exp\left\{-\frac{\|\boldsymbol{x} - \boldsymbol{x}'\|^2}{2\varepsilon^2}\right\} f(\boldsymbol{x}) dx_n \cdots dx_1 \\
&= \frac{1}{(2\pi\varepsilon^2)^{n/2}} \int_{-\infty}^{+\infty} \exp\left\{-\frac{(x_1 - x_1')^2}{2\varepsilon^2}\right\} \cdots \int_{-\infty}^{+\infty} \exp\left\{-\frac{(x_n - x_n')^2}{2\varepsilon^2}\right\} f(\boldsymbol{x}) dx_n \cdots dx_1.
\end{aligned}$$

Again let $s_i = \dfrac{(x_i - x_i') - \frac{x_{i,1}+x_{i,2}}{2}}{\sqrt{2}\varepsilon}$, and furthermore $\xi_i = s_i + \dfrac{x_{i,1} + x_{i,2}}{2}, i = \{1, 2, \ldots, n\}$. We denote $\boldsymbol{x_1} = (x_{1,1}, x_{2,1}, \ldots, x_{n,1})$, $\boldsymbol{x_2} = (x_{1,2}, x_{2,2}, \ldots, x_{n,2})$ and $\boldsymbol{x}' = (x_1', x_2' \ldots, x_n')$. By Taylor Expansion, $f(\boldsymbol{x})$ can be rewritten as

$$\begin{aligned}
f(\boldsymbol{x}) &= f\left(\sqrt{2}\varepsilon \boldsymbol{s} + \frac{\boldsymbol{x_1} + \boldsymbol{x_2}}{2} + \boldsymbol{x}'\right) \\
&= f(\boldsymbol{x}') + \nabla f(\boldsymbol{x}') \left(\sqrt{2}\varepsilon \boldsymbol{s} + \frac{\boldsymbol{x_1} + \boldsymbol{x_2}}{2}\right)
\end{aligned}$$

$$
\begin{aligned}
&+\ \frac{1}{2!}\left(\sqrt{2}\varepsilon \boldsymbol{s}+\frac{\boldsymbol{x_1}+\boldsymbol{x_2}}{2}\right)^T \boldsymbol{H}(\boldsymbol{x}')\left(\sqrt{2}\varepsilon \boldsymbol{s}+\frac{\boldsymbol{x_1}+\boldsymbol{x_2}}{2}\right)+\mathcal{O}(\varepsilon^3)\\
&= f(\boldsymbol{x}')+\nabla f(\boldsymbol{x}')\sqrt{2}\varepsilon\left(\boldsymbol{s}+\frac{\boldsymbol{x_1}+\boldsymbol{x_2}}{2\sqrt{2}\varepsilon}\right)\\
&+\ \varepsilon^2\left(\boldsymbol{s}+\frac{\boldsymbol{x_1}+\boldsymbol{x_2}}{2\sqrt{2}\varepsilon}\right)^T \boldsymbol{H}\left(\boldsymbol{x}')(\sqrt{2}\varepsilon \boldsymbol{s}+\frac{\boldsymbol{x_1}+\boldsymbol{x_2}}{2\sqrt{2}\varepsilon}\right)+\mathcal{O}(\varepsilon^3)\\
&= f(\boldsymbol{x}')+\nabla f(\boldsymbol{x}')\sqrt{2}\varepsilon\boldsymbol{\xi}+\varepsilon^2\boldsymbol{\xi}^T\boldsymbol{H}(\boldsymbol{x}')\boldsymbol{\xi}+\mathcal{O}(\varepsilon^3)
\end{aligned}
$$

where $\boldsymbol{H}(\boldsymbol{x}')$ is Hessian matrix of $f(\boldsymbol{x})$. For any non-negative integer d,

$$
\int_{-\infty}^{+\infty} z^d e^{-z^2}dz=\begin{cases}0, & \text{if } d \text{ is odd,}\\ \Gamma\left(\dfrac{d+1}{2}\right), & \text{if } d \text{ is even.}\end{cases}
$$

First we calculate

$$
\begin{aligned}
&\int_{\mathbb{R}^n}\delta_\varepsilon(\boldsymbol{x}-\boldsymbol{x}')f(\boldsymbol{x})d\Omega\\
&=\frac{1}{(2\pi\varepsilon^2)^{n/2}}\int_{-\infty}^{+\infty}\exp\left\{-\frac{(x_1-x_1')^2}{2\varepsilon^2}\right\}\cdots\int_{-\infty}^{+\infty}\exp\left\{-\frac{(x_n-x_n')^2}{2\varepsilon^2}\right\}f(\boldsymbol{x})dx_n\cdots dx_1\\
&=\frac{1}{\pi^{n/2}}\int_{-\infty}^{+\infty}\exp\left\{\left(-s_1+\frac{x_{1,1}+x_{1,2}}{2}\right)^2\right\}\cdots\int_{-\infty}^{+\infty}\exp\left\{\left(-s_n+\frac{x_{n,1}+x_{n,2}}{2}\right)^2\right\}\\
&f\left(\sqrt{2}\varepsilon\boldsymbol{s}+\frac{\boldsymbol{x_1}+\boldsymbol{x_2}}{2}+\boldsymbol{x}'\right)ds_n\cdots ds_1\\
&=\frac{1}{\pi^{n/2}}\int_{-\infty}^{+\infty}e^{-\xi_1^2}\cdots\int_{-\infty}^{+\infty}e^{-\xi_n^2}f(\sqrt{2}\varepsilon\boldsymbol{\xi}+\boldsymbol{x}')d\xi_n\cdots d\xi_1\\
&=\frac{1}{\pi^{n/2}}\int_{-\infty}^{+\infty}e^{-\xi_1^2}\cdots\int_{-\infty}^{+\infty}e^{-\xi_n^2}[f(\boldsymbol{x}')+\nabla f(\boldsymbol{x}')\sqrt{2}\varepsilon\boldsymbol{\xi}+\varepsilon^2\boldsymbol{\xi}^T\boldsymbol{H}(\boldsymbol{x}')\boldsymbol{\xi}+\mathcal{O}(\varepsilon^3)]d\xi_n\cdots d\xi_1\\
&=\frac{f(\boldsymbol{x}')}{\pi^{n/2}}\int_{-\infty}^{+\infty}e^{-\xi_1^2}\cdots\int_{-\infty}^{+\infty}e^{-\xi_n^2}d\xi_n\cdots d\xi_1\\
&+\ \frac{\sqrt{2}\varepsilon}{\pi^{n/2}}\int_{-\infty}^{+\infty}e^{-\xi_1^2}\xi_1 f'_{x_1}(\boldsymbol{x}')\cdots\int_{-\infty}^{+\infty}e^{-\xi_n^2}\xi_n f'_{x_n}(\boldsymbol{x}')d\xi_n\cdots d\xi_1\\
&+\ \frac{\varepsilon^2}{\pi^{n/2}}\int_{-\infty}^{+\infty}e^{-\xi_1^2}(\sqrt{2}\xi_1+f''_{x_1,x_1}(\boldsymbol{x}'))\xi_1^2\\
&+\ \sum_{i=1,i\neq 1}^{n} f''_{x_1,x_i}(\boldsymbol{x}')\xi_1\xi_i\cdots\int_{-\infty}^{+\infty}e^{-\xi_n^2}(\sqrt{2}\xi_1+(f''_{x_n,x_n})(\boldsymbol{x}'))\xi_n^2\\
&+\ \sum_{i=1,i\neq n}^{n} f''_{x_n,x_i}(\boldsymbol{x}')\xi_n\xi_i d\xi_n\cdots d\xi_1+\mathcal{O}(\varepsilon^3)\\
&= f(\boldsymbol{x}')+\frac{\varepsilon^2}{\sqrt{\pi}}\Gamma\left(\frac{3}{2}\right)\sum_{i=1}^{d} f''_{x_i,x_i}(\boldsymbol{x}')+\mathcal{O}(\varepsilon^3)\to f(\boldsymbol{x}'),
\end{aligned}
$$

as $\varepsilon\to 0^+$.

For the integral over the given domain $\Omega=(x_{1,1},x_{1,2})\times\cdots\times(x_{n,1},x_{n,2})$, it can be written as

$$
\begin{aligned}
&\int_{x_{1,1}}^{x_{1,2}}\cdots\int_{x_{n,1}}^{x_{n,2}}dx_n\cdots dx_1=\int_{-\infty}^{+\infty}\cdots\int_{-\infty}^{+\infty}dx_n\cdots dx_1\\
&-\ \sum_{i=1}^{n}\int_{x_{1,1}}^{x_{1,2}}\cdots\int_{-\infty}^{x_{i,1}}\cdots\int_{x_{n,1}}^{x_{n,2}}dx_n\cdots dx_1-\sum_{i=1}^{n}\int_{x_{1,1}}^{x_{1,2}}\cdots\int_{x_{i,2}}^{+\infty}\cdots\int_{x_{n,1}}^{x_{n,2}}dx_n\cdots dx_1
\end{aligned}
$$

$$= (\sqrt{2}\varepsilon)^n \left[\int_{-\infty}^{+\infty}\cdots\int_{-\infty}^{+\infty} ds_n\cdots ds_1\right.$$
$$\left. -\sum_{i=1}^{n}\int_{s_{1,1}}^{s_{1,2}}\cdots\int_{-\infty}^{s_{i,1}}\cdots\int_{s_{n,1}}^{s_{n,2}} ds_n\cdots ds_1 - \sum_{i=1}^{n}\int_{\xi_{1,1}}^{\xi_{1,2}}\cdots\int_{\xi_{i,2}}^{+\infty}\cdots\int_{\xi_{n,1}}^{\xi_{n,2}} d\xi_n\cdots d\xi_1\right]$$
$$= (\sqrt{2}\varepsilon)^n \left[\int_{-\infty}^{+\infty}\cdots\int_{-\infty}^{+\infty} d\xi_n\cdots d\xi_1\right.$$
$$\left. -\sum_{i=1}^{n}\int_{\xi_{1,1}}^{\xi_{1,2}}\cdots\int_{-\infty}^{\xi_{i,1}}\cdots\int_{\xi_{n,1}}^{\xi_{n,2}} d\xi_n\cdots d\xi_1 - \sum_{i=1}^{n}\int_{\xi_{1,1}}^{\xi_{1,2}}\cdots\int_{\xi_{i,2}}^{+\infty}\cdots\int_{\xi_{n,1}}^{\xi_{n,2}} d\xi_n\cdots d\xi_1\right],$$

where $\xi_{i,1} = \dfrac{x_{i,1}-x_i'}{\sqrt{2}\varepsilon}$ and $\xi_{i,2} = \dfrac{x_{i,2}-x_i'}{\sqrt{2}\varepsilon}$. Therefore,

$$\left|\int_\Omega \delta_\varepsilon(\boldsymbol{x}-\boldsymbol{x}')f(\boldsymbol{x})d\Omega - f(\boldsymbol{x}')\right|$$
$$= \left| f(\boldsymbol{x}') + \frac{\varepsilon^2}{\sqrt{\pi}}\Gamma\left(\frac{3}{2}\right)\sum_{i=1}^{d} f''_{x_i,x_i}(\boldsymbol{x}') + \mathcal{O}(\varepsilon^3) - \frac{1}{\pi^{n/2}}\left[\sum_{i=1}^{n}\int_{\xi_{1,1}}^{\xi_{1,2}} e^{-\xi_1}\cdots\int_{-\infty}^{\xi_{i,1}} e^{-\xi_i}\right.\right.$$
$$\cdots\int_{\xi_{n,1}}^{\xi_{n,2}} e^{-\xi_n} f(\sqrt{2}\varepsilon\boldsymbol{\xi}+\boldsymbol{x}')d\xi_n\cdots d\xi_1 + \sum_{i=1}^{n}\int_{\xi_{1,1}}^{\xi_{1,2}} e^{-\xi_1}\cdots\int_{\xi_{i,2}}^{+\infty} e^{-\xi_i}$$
$$\left.\left.\cdots\int_{\xi_{n,1}}^{\xi_{n,2}} e^{-\xi_n} f(\sqrt{2}\varepsilon\boldsymbol{\xi}+\boldsymbol{x}')d\xi_n\cdots d\xi_1\right] - f(\boldsymbol{x}')\right|$$
$$\leqslant \left|\frac{\varepsilon^2}{\sqrt{\pi}}\Gamma\left(\frac{3}{2}\right)\sum_{i=1}^{d} f''_{x_i,x_i}(\boldsymbol{x}') + \mathcal{O}(\varepsilon^3)\right|$$
$$+ \frac{M}{2^{n-1}}\sum_{j=1}^{n}\prod_{i=1,i\neq j}^{n}[\mathrm{erf}(\xi_{j,2}) - \mathrm{erf}(\xi_{j,1}) + 2]\times[\mathrm{erf}(\xi_{i,2}) - \mathrm{erf}(\xi_{i,1})]$$
$$\leqslant \left|\frac{\varepsilon^2}{\sqrt{\pi}}\Gamma\left(\frac{3}{2}\right)\sum_{i=1}^{d} f''_{x_i,x_i}(\boldsymbol{x}') + \mathcal{O}(\varepsilon^3)\right| + \frac{M}{2}\sum_{j=1}^{n}[\mathrm{erf}(\xi_{j,1}) - \mathrm{erf}(\xi_{j,2}) + 2]$$
$$\to 0, \text{ as } \varepsilon \to 0^+,$$

since $\|f(\boldsymbol{x})\| < M < +\infty$, $\xi_{i,1} \to -\infty$ and $\xi_{i,2} \to \infty$ respectively. Using $1 - \mathrm{erf}(y) < \dfrac{2}{\sqrt{\pi}}\exp(-y)$ for $y > 0$ and the fact that $\exp(y) < \dfrac{1}{y^\alpha}$ as $y \to \infty$, we see that the second term approximates zero faster than the first term. Hence, we conclude that there is a $C > 0$ such that

$$\left|\int_\Omega \delta_\varepsilon(\boldsymbol{x}-\boldsymbol{x}')f(\boldsymbol{x})d\Omega - f(\boldsymbol{x}')\right| \leqslant C\varepsilon^2 \text{ as } \varepsilon \to 0^+. \quad \square$$

As a remark we add that setting $f(\boldsymbol{x}) = 1$, immediately shows that there is a $C > 0$ such that

$$\left|\int_\Omega \delta_\varepsilon(\boldsymbol{x}-\boldsymbol{x}')d\Omega - 1\right| \leqslant C\varepsilon^2, \text{ as } \varepsilon \longrightarrow 0^+.$$

Furthermore, the above results are stronger than the convergence in distribution of the Gaussian to the Dirac Delta distribution. Using the result above, we start with analysing different approaches with only one relatively big cell in the computational domain. According to the model described in Eq. (8), the forces released on the boundary of the cell are the superposition of point forces on the midpoint of each surface element. For example, if we use a square shape to approximate the biological cell, then the forces are depicted in Fig. 1. Therefore, in n dimensional

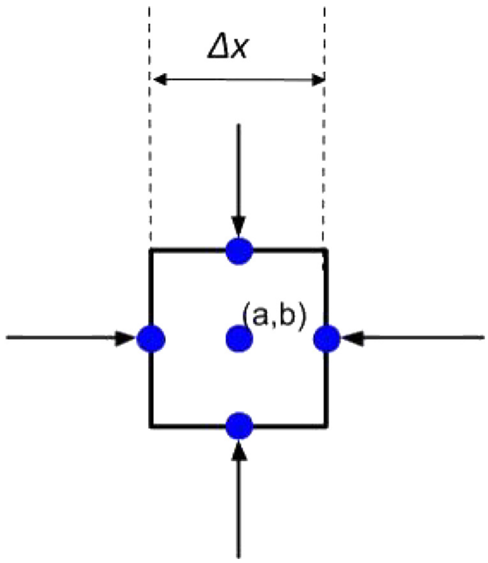

Fig. 1. We consider a square shape cell in two dimensions, with the centre position at (a, b) and side length Δx. The forces exerted on the boundary are indicated by arrows.

case ($n > 1$), if the biological cell is a n-dimensional hypercube, then the forces can be rewritten as

$$\begin{aligned} \boldsymbol{f}_t &= \sum_{j=1}^{N_S} P(\boldsymbol{x}_j)\boldsymbol{n}(\boldsymbol{x}_j)\delta(\boldsymbol{x}-\boldsymbol{x}_j)\Delta S(\boldsymbol{x}_j) \\ &= P\sum_{i=1}^{n}\{\boldsymbol{e_i}(\Delta x)^{n-1}[\delta(x_1 - x_1', \ldots, x_i - (x_i' + \frac{\Delta x}{2}), \ldots, x_n - x_n') \\ &- \delta(x_1 - x_1', \ldots, x_i - (x_i' - \frac{\Delta x}{2}), \ldots, x_n - x_n')]\}, \end{aligned} \tag{13}$$

where $\boldsymbol{e_i}$ is the standard basis vector with 1 in the ith coordinate and $0's$ elsewhere, and Δx is the length of cell boundary in each coordinate. For the smoothed force approach, we set $\delta(\boldsymbol{x}) \approx \delta_\varepsilon(\boldsymbol{x})$. The force is given by

$$\begin{aligned} \boldsymbol{f}_\varepsilon = P\sum_{i=1}^{n}\{\boldsymbol{e_i}(\Delta x)^{n-1}[\delta_\varepsilon(x_1 - x_1', \ldots, x_i - (x_i' + \frac{\Delta x}{2}), \ldots, x_n - x_n') \\ - \delta_\varepsilon(x_1 - x_1', \ldots, x_i - (x_i' - \frac{\Delta x}{2}), \ldots, x_n - x_n')]\}. \end{aligned} \tag{14}$$

Following the same process in two dimensions [17] and thanks to the continuity of Gaussian distribution, as $\Delta x \to 0$, the force converges to

$$\boldsymbol{f}_S = P(\Delta x)^n \nabla\delta_\varepsilon(\boldsymbol{x} - \boldsymbol{x}'). \tag{15}$$

Theorem 3. *Let $\Omega \subset \mathbb{R}^n$, and let $\mathbf{V}_h(\Omega) \subset \mathbf{H}_0^1(\Omega)$, and suppose that $\boldsymbol{u}_h \subset \boldsymbol{V}_h(\Omega)$ is the Galerkin solution to the problem*

$$(BVP)\begin{cases} \text{Find } \boldsymbol{u}_h \in \boldsymbol{V}_h(\Omega) \text{ such that} \\ a(\boldsymbol{u}_h, \boldsymbol{\phi}_h) = \int_\Omega \boldsymbol{f}_t \boldsymbol{\phi}_h d\Omega, \text{for all } \boldsymbol{\phi}_h \in \boldsymbol{V}_h(\Omega), \end{cases} \tag{16}$$

and let $\boldsymbol{u}_h^{\boldsymbol{\varepsilon}}$ *be the Galerkin solution to*

$$(BVP_{\varepsilon})\begin{cases}\text{Find } \boldsymbol{u}_h^{\varepsilon} \in \boldsymbol{V}_h(\Omega) \text{ such that}\\ a(\boldsymbol{u}_h^{\varepsilon}, \boldsymbol{\phi}_h) = \int_{\Omega} \boldsymbol{f}_{\varepsilon}\boldsymbol{\phi}_h d\Omega, \text{for all } \boldsymbol{\phi}_h \in \boldsymbol{V}_h(\Omega).\end{cases} \tag{17}$$

Then there is an $L_1 > 0$ *such that* $\|\boldsymbol{u}_h^{\boldsymbol{\varepsilon}} - \boldsymbol{u}_h\|_{\boldsymbol{H}^1(\Omega)} \leqslant L_1\ (\Delta x)^{(n-1)/2}\ \varepsilon$.

Proof. Using bilinearity of $a(.,.)$ gives upon setting $\boldsymbol{w} = \boldsymbol{u}_h - \boldsymbol{u}_h^{\boldsymbol{\varepsilon}}$ the following equation:

$$a(\boldsymbol{w}, \boldsymbol{\phi}_h) = \int_{\Omega} (\boldsymbol{f}_t - \boldsymbol{f}_{\epsilon}) \cdot \boldsymbol{\phi}_h d\Omega.$$

Using the result from Lemma 3 and the Triangle Inequality, bearing in mind that $\|\boldsymbol{e}_i\| = 1$ and that the basis field functions $\boldsymbol{\phi}_h$ are bounded, and after some algebraic manipulations, we can write the right-hand side as

$$\left|\int_{\Omega} (\boldsymbol{f}_t - \boldsymbol{f}_{\epsilon}) \cdot \boldsymbol{\phi}_h d\Omega\right| \leqslant C(\Delta x)^{n-1}\varepsilon^2. \tag{18}$$

Coerciveness, see Lemma 2, and using $\boldsymbol{\phi}_h = \boldsymbol{w}$, gives

$$K\|\boldsymbol{w}\|^2_{H_1(\Omega)} \leqslant a(\boldsymbol{w}, \boldsymbol{w}) \leqslant C(\Delta x)^{n-1}\varepsilon^2,$$

hence there is an $L_1 > 0$ such that

$$\|\boldsymbol{w}\|_{H_1(\Omega)} \leqslant L\ (\Delta x)^{(n-1)/2}\ \varepsilon,$$

which immediately implies that

$$\|\boldsymbol{u}_h - \boldsymbol{u}_h^{\varepsilon}\|_{H_1(\Omega)} \leqslant L_1\ (\Delta x)^{(n-1)/2}\ \varepsilon \quad \square$$

Theorem 4. *Let* $\Omega \subset \mathbb{R}^n$, *and let* $\mathbf{V}_h(\Omega) \subset \mathbf{H}_0^1(\Omega)$, *and suppose that* $\boldsymbol{u}_h^{\boldsymbol{\varepsilon}}$ *is the solution to the boundary value problems in Eq. (17), and let* $\boldsymbol{u}_h^S$ *be the solution to*

$$(BVP_{SP})\begin{cases}\text{Find } \boldsymbol{u}_h^{\varepsilon} \in \boldsymbol{V}_h(\Omega) \text{ such that}\\ a(\boldsymbol{u}_h^{\varepsilon}, \boldsymbol{\phi}_h) = \int_{\Omega} \boldsymbol{f}_S\boldsymbol{\phi}_h d\Omega, \text{for all } \boldsymbol{\phi}_h \in \boldsymbol{V}_h(\Omega).\end{cases} \tag{19}$$

Then there is an $L_2 > 0$ *such that*

$$\frac{1}{(\Delta x)^n}\|\boldsymbol{u}_h^S - \boldsymbol{u}_h^{\epsilon}\|_{\boldsymbol{H}^1(\Omega)} \leqslant L_2\frac{(\Delta x)^2}{\varepsilon^3}.$$

Proof. Using bilinearity of $a(.,.)$ gives, upon setting $\boldsymbol{w} = \boldsymbol{u}_h^{\varepsilon} - \boldsymbol{u}_h^S$, the following equation:

$$a(\boldsymbol{w}, \boldsymbol{\phi}_h) = \int_{\Omega} (\boldsymbol{f}_{\varepsilon} - \boldsymbol{f}_S) \cdot \boldsymbol{\phi}_h d\Omega.$$

Using Taylor's Theorem for multivariate functions on smoothed delta distributions, we get the following result for the right-hand side:

$$\int_{\Omega} (\boldsymbol{f}_{\epsilon} - \boldsymbol{f}_S) \cdot \boldsymbol{\phi}_h d\Omega = \int_{\Omega} \frac{P(\boldsymbol{x}')}{48}(\Delta x)^{n+2}\sum_{i=1}^{n} \boldsymbol{e}_i \frac{\partial^3 \delta_{\epsilon}(\hat{\boldsymbol{x}} - \boldsymbol{x}')}{\partial x_i^3} \cdot \boldsymbol{\phi}_h d\Omega, \tag{20}$$

for $\hat{\boldsymbol{x}}$ between $\boldsymbol{x}$ and $\boldsymbol{x}'$. The magnitude of the above expression can be estimated from above by

$$\left|\int_{\Omega} (\boldsymbol{f}_{\epsilon} - \boldsymbol{f}_S) \cdot \boldsymbol{\phi}_h d\Omega\right| \leqslant \frac{P(\boldsymbol{x}')}{48}(\Delta x)^{n+2}\left\|\sum_{i=1}^{n} \boldsymbol{e}_i \frac{\partial^3 \delta_{\epsilon}}{\partial x_i^3}\right\|_{L^{\infty}(\Omega)} \|\boldsymbol{\phi}_h\|_{\boldsymbol{H}^1(\Omega)}. \tag{21}$$

Using Lemma 2, this gives

$$K\|\boldsymbol{w}\|^2_{\boldsymbol{H}^1(\Omega)} \leqslant a(\boldsymbol{w}, \boldsymbol{w}) \leqslant \frac{P(\boldsymbol{x}')}{48}(\Delta x)^{n+2}\left\|\sum_{i=1}^{n} \boldsymbol{e}_i \frac{\partial^3 \delta_{\epsilon}}{\partial x_i^3}\right\|_{L^{\infty}(\Omega)} \|\boldsymbol{\phi}_h\|_{\boldsymbol{H}^1(\Omega)}.$$

Table 1
Parameter values used in the comparison of plasticity and morphoelasticity.

Parameter	Description	Value
E	Substrate stiffness	1
β	Factor between the cell stiffness and the substrate stiffness in Eq (11)	10^{-5}
R	Length of side of square-shape biological cells	6
ν	Poisson's ratio	0.48
P	Magnitude of the temporary forces per unit length	1
x_0	Length of the computational domain in x-coordinate	20
y_0	Length of the computational domain in y-coordinate	20
w_x	Length of the wound domain in x-coordinate	10
w_y	Length of the wound domain in y-coordinate	10

Division by $K\|\boldsymbol{w}\|^2_{\boldsymbol{H^1}(\Omega)}$ gives

$$\|\boldsymbol{w}\|_{\boldsymbol{H^1}(\Omega)} \leqslant \frac{P(\boldsymbol{x}')}{48}(\Delta x)^{n+2}\left\|\sum_{i=1}^{n}\boldsymbol{e}_i\frac{\partial^3\delta_\epsilon}{\partial x_i^3}\right\|_{L^\infty(\Omega)}.$$

We bear in mind that $\frac{\partial^3\delta_\epsilon}{\partial x_i^3} = \mathcal{O}(\varepsilon^{-3})$, this implies that there is an $L_2 > 0$ such that

$$\frac{1}{(\Delta x)^n}\|\boldsymbol{u}_h^S - \boldsymbol{u}_h^\epsilon\|_{\boldsymbol{H^1}(\Omega)} \leqslant L_2\frac{(\Delta x)^2}{\varepsilon^3}. \quad \square$$

With the two theorems above, we have proved that the solution to (BVP_ε) converges to the solution to (BVP), and the solution to (BVP_{SP}) converges to the solution to (BVP_ε). Hence, we can derive the following theorem:

Theorem 5. *Let $\Omega \subset \mathbb{R}^n$, and let $\mathbf{V}_h(\Omega) \subset \mathbf{H}_0^1(\Omega)$, and suppose that $\boldsymbol{u}_h$ is the Galerkin solution to (BVP) and let $\boldsymbol{u}_h^S$ be the solution to (BVP_{SP}), let $\varepsilon = \mathcal{O}(\Delta x)^p$. If $0 < p < (2+n)/3$ then $\boldsymbol{u}_h^S$ converges to $\boldsymbol{u}_h$ in the H^1-norm, and $\boldsymbol{u}_h^S$ converges to $\boldsymbol{u}$ in the H^1-norm as $\Delta x \longrightarrow 0$..*

Proof. Denote $\boldsymbol{u}_h$ and $\boldsymbol{u}_h^S$ to be the Galerkin solution to (BVP_ε) and (BVP_{SP}). Firstly, we consider

$$\begin{aligned}
\|\boldsymbol{u}_h - \boldsymbol{u}_h^S\| &= \|\boldsymbol{u}_h - \boldsymbol{u}_h^{\boldsymbol{\varepsilon}} + \boldsymbol{u}_h^{\boldsymbol{\varepsilon}} - \boldsymbol{u}_h^S\| \\
&\leqslant \|\boldsymbol{u}_h - \boldsymbol{u}_h^{\boldsymbol{\varepsilon}}\| + \|\boldsymbol{u}_h^{\boldsymbol{\varepsilon}} - \boldsymbol{v}_h^{\boldsymbol{\varepsilon}}\| \\
&\leqslant L_1(\Delta x)^{(n-1)/2}\varepsilon + L_2\frac{(\Delta x)^{2+n}}{\varepsilon^3} \\
&= L_1(\Delta x)^{(n-1)/2+p} + L_2(\Delta x)^{2+n-3p} \to 0, \\
&\text{as } \Delta x \to 0, \text{ if } 0 < p < (2+n)/3.
\end{aligned}$$

From this inequality, we conclude that the finite element solution of the smooth particle method converges to the solution of the immersed boundary method upon letting $\Delta x \to 0$ and choosing $\varepsilon = \mathcal{O}(\Delta x)^p$ for $0 < p < (2+p)/3$. $\square$

4. Numerical results in two dimensions

To demonstrate the consistency between the immersed boundary approach and two alternative methods, we consider a square-shape cell in the computational domain. A homogeneous boundary condition is imposed for the exterior boundary of the computational domain. The parameter values are listed in Table 1. All of them are educated guesses in this study and they are dimensionless.

According to Proposition 1, to compare the immersed boundary approach and the 'hole' approach, the stiffness inside the biological cell needs to be adjusted, since two approaches are consistent with $\beta \to 0$. However, in the implementation, we can only select a very small positive value instead of $\beta = 0$.

Numerical results are presented in Fig. 2, Tables 2 and 3. From the figure, there is no significant difference, except that in the smoothed particle approach, the displacement is a little bit larger than in the other two approaches. The

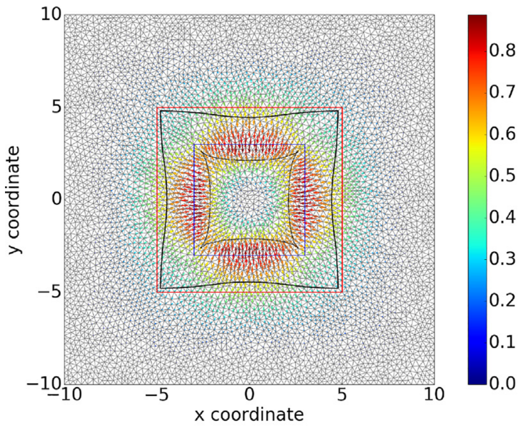

(a) Immersed boundary approach

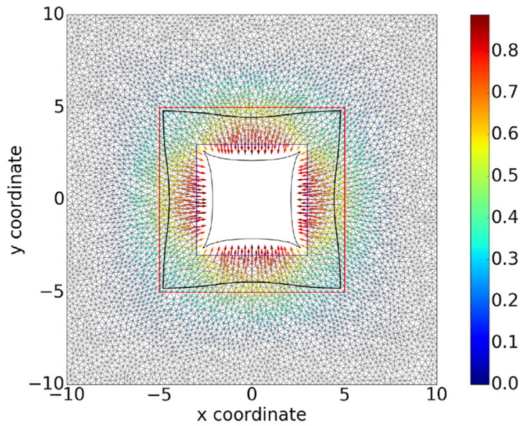

(b) The 'hole' approach

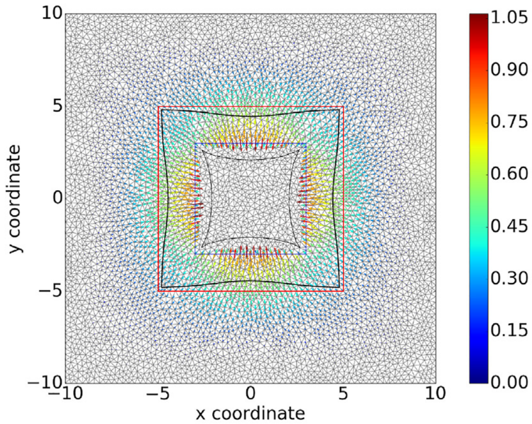

(c) Smoothed particle approach

Fig. 2. For the different stiffness inside and outside of the cell, the solution (i.e. the displacement) is showed in each approach. Black curves show the deformed region of vicinity and the cell, and blue curve represents the cell. (For interpretation of the references to colour in this figure legend, the reader is referred to the web version of this article.)

Table 2
The percentage of area change of cell and vicinity region, and time cost of various approaches, if the stiffness is different inside and outside the biological cell.

	The immersed boundary approach	The 'hole' approach	The smoothed particle approach
Cell Area Reduction Ratio (%)	45.84096	45.71401	45.18525
Vicinity Area Reduction Ratio (%)	14.274671	14.15804	14.16180
Time Cost (s)	0.78643	1.10195	0.75832

reduction ratio of either the vicinity region or the cell appears to yield a tiny difference, which implies that three approaches are numerically consistent. However, the 'hole' approach takes slightly more computation time than the other two approaches. Therefore and due to the numerical complications in needing adaptive meshes, it will not be elected when we deal with the displacement and deformation of large number of cells, even though its convergence rate improves significantly comparing to the immersed boundary approach. As for the smoothed particle approach, the convergence rate of the L_2-norm does not improve, while the computational efficiency does.

Table 3
The $L^2 - norm$ of the solution (i.e. the displacement) with different mesh size in each approach, if the stiffness is different inside and outside the biological cell.

	The immersed boundary approach	The 'hole' approach	The smoothed particle approach
h	5.8833092	5.9256424	5.8981846
h/2	5.9302898	5.952170	5.9324678
h/4	5.9484929	5.9593735	5.9486686
Convergence rate	1.36788	1.88060	1.08102

5. Conclusion

For dimensionalities larger than one, the solution to the displacement from linear elasticity with Dirac Delta distributions is singular. We analyse the solutions based on Galerkin approximations with Lagrangian basis functions for different approaches that are consistent if cell sizes and smoothness parameters tend to zero. We have shown that all the alternative approaches are numerically consistent with the immersed boundary approach. The current paper has investigated and extended earlier findings to multi dimensionality. The current analysis has been carried out for simple, linear elasticity. Using the fundamental solution to the elasticity equation in two and three dimensions, as well as the singularity removing technique, we expect that it is also possible to extend some of our results to the (non Galerkin-based) exact solution to the elasticity problem. In the future, we plan to extend our findings to the viscoelasticity equations. This viscoelastic model contains a damping term, and still retains a linear nature. Furthermore, we are also interested in analysing the above considered principles for a morphoelastic model. A morphoelastic model has the major advantage of incorporating permanent deformations. A major complication is its nonlinear nature.

Declaration of competing interest

The authors declare that they have no known competing financial interests or personal relationships that could have appeared to influence the work reported in this paper.

References

[1] U. Andreaus, F. dell'Isola, I. Giorgio, L. Placidi, T. Lekszycki, N.L. Rizzi, Numerical simulations of classical problems in two-dimensional (non) linear second gradient elasticity, Internat. J. Engrg. Sci. 108 (2016) 34–50, http://dx.doi.org/10.1016/j.ijengsci.2016.08.003.
[2] K. Atkinson, W. Han, Theoretical Numerical Analysis, Vol. 39, Springer, 2005.
[3] J. Berger, A. Karageorghis, The method of fundamental solutions for layered elastic materials, Eng. Anal. Bound. Elem. 25 (10) (2001) 877–886, http://dx.doi.org/10.1016/s0955-7997(01)00002-9.
[4] S. Bertoluzza, A. Decoene, L. Lacouture, S. Martin, Local error estimates of the finite element method for an elliptic problem with a Dirac source term, Numer. Methods Partial Differential Equations 34 (1) (2018) 97–120.
[5] W. Boon, D. Koppenol, F. Vermolen, A multi-agent cell-based model for wound contraction, J. Biomech. 49 (8) (2016) 1388–1401.
[6] D. Braess, Finite Elements: Theory, Fast Solvers, and Applications in Solid Mechanics, Cambridge University Press, 2007.
[7] C. D'Angelo, Finite element approximation of elliptic problems with Dirac measure terms in weighted spaces: Applications to one- and three-dimensional coupled problems, SIAM J. Num. Anal. 50 (1) (2012) 194–215, http://dx.doi.org/10.1137/100813853.
[8] M.J. Eichler, M.A. Carlson, Modeling dermal granulation tissue with the linear fibroblast-populated collagen matrix: a comparison with the round matrix model, J. Dermatol. Sci. 41 (2) (2006) 97–108.
[9] S. Enoch, D.J. Leaper, Basic science of wound healing, Surg. (Oxford) 26 (2) (2008) 31–37.
[10] I.G. Gjerde, K. Kumar, J.M. Nordbotten, A singularity removal method for coupled 1D–3D flow models, Comput. Geosci. 24 (2) (2019) 443–457, http://dx.doi.org/10.1007/s10596-019-09899-4.
[11] E. Haertel, S. Werner, M. Schäfer, Transcriptional regulation of wound inflammation, in: Seminars in Immunology, Vol. 26, (4) Elsevier, 2014, pp. 321–328.
[12] D. Koppenol, Biomedical implications from mathematical models for the simulation of dermal wound healing, (PhD-Thesis), At the Delft University of Technology, the Netherlands, 2017.
[13] T. Köppl, B. Wohlmuth, Optimal a priori error estimates for an elliptic problem with Dirac right-hand side, SIAM J. Num. Anal. 52 (4) (2014) 1753–1769, http://dx.doi.org/10.1137/130927619.
[14] L. Lacouture, A numerical method to solve the Stokes problem with a punctual force in source term, Comp. Rendus MÉCanique 343 (3) (2015) 187–191.

[15] B. Li, J.H.-C. Wang, Fibroblasts and myofibroblasts in wound healing: force generation and measurement, J. Tissue Viability 20 (4) (2011) 108–120.
[16] Q. Peng, F. Vermolen, Numerical Methods to Solve Elasticity Problems with Point Sources, Reports of the Delft Institute of Applied Mathematics, (19–02) Delft University of Technology, Delft, the Netherlands, 2019, pp. 1389–6520.
[17] Q. Peng, F. Vermolen, Point Forces and Their Alternatives in Cell-Based Models for Skin Contraction, Reports of the Delft Institute of Applied Mathematics, Delft University of Technology, Delft, the Netherlands, 2019, pp. 1389–6520, 19–03.
[18] L. Placidi, A variational approach for a nonlinear 1-dimensional second gradient continuum damage model, Contin. Mech. Thermodyn. 27 (4–5) (2014) 623–638, http://dx.doi.org/10.1007/s00161-014-0338-9.
[19] F. Putar, J. Sorić, T. Lesičar, Z. Tonković, Damage modeling employing strain gradient continuum theory, Int. J. Solids Struct. 120 (2017) 171–185, http://dx.doi.org/10.1016/j.ijsolstr.2017.04.039.
[20] J.C. Reiher, I. Giorgio, A. Bertram, Finite-element analysis of polyhedra under point and line forces in second-strain gradient elasticity, J. Eng. Mech. 143 (2) (2017) 04016112, http://dx.doi.org/10.1061/(asce)em.1943-7889.0001184.
[21] R. Scott, Finite element convergence for singular data, Numer. Math. 21 (4) (1973) 317–327.
[22] F. Vermolen, A. Gefen, Semi-stochastic cell-level computational modelling of cellular forces: Application to contractures in burns and cyclic loading, Biomech. Model. Mechanobiol. 14 (6) (2015) 1181–1195.
[23] Y. Yang, A. Misra, Micromechanics based second gradient continuum theory for shear band modeling in cohesive granular materials following damage elasticity, Int. J. Solids Struct. 49 (18) (2012) 2500–2514, http://dx.doi.org/10.1016/j.ijsolstr.2012.05.024.